

Excited-State Electron Transfer in Anthocyanins and Related Flavylium Salts

Palmira Ferreira da Silva,[†] João C. Lima,[‡] Frank H. Quina,[§] and Antonio L. Maçanita^{*,†}

Centro de Química Estrutural, Departamento de Engenharia Química, IST/UTL, Lisbon, Portugal, Centro de Química Fina e Biotecnologia, Departamento Química, FCT/UNL, Portugal, and Instituto de Química, Universidade de São Paulo, CP 26077, São Paulo 05513-970, Brazil

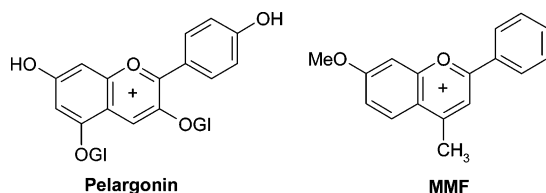
Received: June 21, 2004; In Final Form: September 3, 2004

Anthocyanins constitute the major red and purple pigments in plants. In this work, it is shown that the red flavylium cation of anthocyanins forms ground-state charge transfer complexes with several naturally occurring electron donors, such as flavones (e.g., quercitrin) and even benzoic and cinnamic acid derivatives. Excitation of these charge transfer complexes results in efficient static fluorescence quenching due to fast electron transfer from the copigment to the flavylium cation. The complete inhibition of the fluorescence of the excited base form of anthocyanin implies that the rate constant for electron transfer is substantially larger than that for deprotonation (ca. 10^{11} s^{-1}). The high efficiency of electron transfer results from the high oxidizing power in the excited state of the red form of anthocyanins. In uncomplexed anthocyanins, ultrafast proton transfer efficiently dissipates the absorbed light energy. Although ultrafast electron transfer could play a similar role in flavylium cation–polyphenol complexes, it may also serve as a source of free radicals if recombination is not 100% efficient, which might eventually be important for understanding the role in vivo of anthocyanin–polyphenol complexes.

Introduction

Anthocyanins impart most of the red and purple colors found in plants.^{1,2} The red color is due to the flavylium cation, AH^+ , (Chart 1), while purple is normally associated with the conjugated quinonoidal form, A, or complexes of AH^+ with other polyphenols or metal ions. Electronic excitation of AH^+ in aqueous solution results in ultrafast proton transfer to water in 5–25 ps.^{4,5} The two strong absorption bands of AH^+ at ca. 500 and 300 nm are complementary to the absorption spectrum of chlorophyll, and ultrafast excited-state proton transfer (ESPT) of AH^+ may provide an efficient dissipation channel for excess absorption of solar energy.

CHART 1



In aqueous solution, AH^+ is stable only at $\text{pH} < 2$. At higher pH values, deprotonation and hydration of AH^+ produce, respectively, a blue-colored quinonoidal base, A, and a colorless hemiacetal, B, which in turn tautomerizes to give two isomeric chalcones, C_E and C_Z (Scheme 1).^{6–9}

Because the value of K_h for hydration of AH^+ is normally ca. 10- to 100-fold larger than K_a , and the $\text{p}K_a$'s of anthocyanins are in the range 4–5, aqueous solutions of anthocyanins typically start losing their color at $\text{pH} > 2$.

The AH^+ form of anthocyanins forms stable complexes with a great number of other natural polyphenols, such as hydroxyl derivatives of benzoic or cinnamic acids and flavones,^{10–13} in which hydration of AH^+ is disfavored. Consequently, in the presence of such compounds (e.g., in plant vacuoles¹⁴) anthocyanins retain their red color at $\text{pH} > 2$. Additionally, AH^+ can be stabilized by self-aggregation or by complexation with the C_Z form.¹⁵

The present work reports a detailed study of complexes between AH^+ and several natural phenols in both the ground and excited states. We provide evidence that AH^+ cations are exceptionally good electron acceptors, leading to ultrafast electron transfer from the polyphenol to the excited state of AH^+ .

Experimental Section

Materials. The anthocyanin pelargonidin-3,5-diglucoside (pelargonin) was purchased from Extrasynthèse and used without further purification. The synthetic anthocyanin 4-methyl-7-methoxyflavylium chloride (MMF) was synthesized and purified as described previously.⁴ The polyphenolic compounds, protocatechuic acid (Aldrich, 97%), quercitrin (Extrasynthèse, HPLC grade), isoquercitrin (Extrasynthèse, HPLC grade), gallic acid (Aldrich, 97%), ferulic acid (Aldrich, 99%), and caffeic acid (Sigma, HPLC grade) were used as received. Water was twice distilled and deionized (Elgastat UHQ PS). Methanol G Chromasolv (Riedel-de-Haën) and acetonitrile UV grade (Fluka) were used as received.

Measurements. The pH was measured at 20 °C with a Crison micropH 2002. UV–vis absorption spectra were recorded on a Beckman DU-70 spectrophotometer.

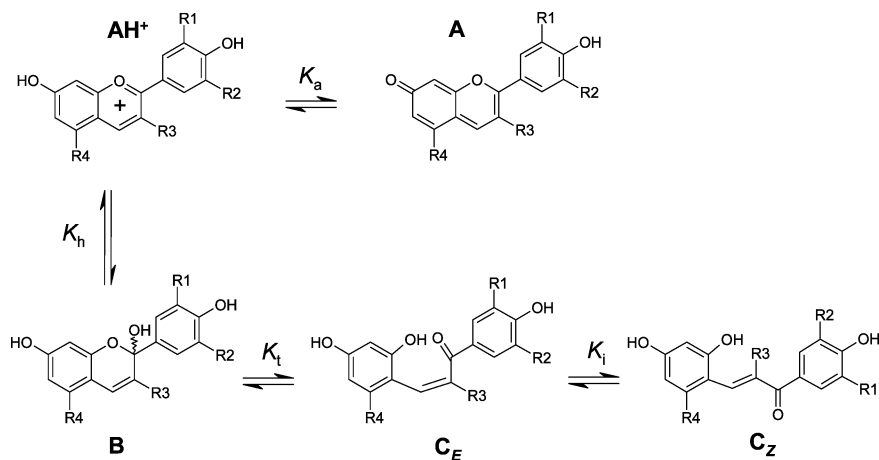
Cyclic voltammetric (CV) measurements were carried out on an AUTOLAB PGSTAT12 potentiostat. The three-electrode system, used in the common triangular configuration, consisted of an Hg suspended drop working electrode (or Pt electrode in

[†] Departamento de Engenharia Química, IST/UTL.

[‡] Departamento Química, FCT/UNL.

[§] Universidade de São Paulo.

SCHEME 1



the case of the protocatechuic acid measurements), a saturated calomel electrode (SCE) (or Ag/AgCl/3.0 M KCl, in the case of pelargonin) reference electrode, and a platinum wire as an auxiliary electrode. The suspended drop Hg electrode was used, because anthocyanins strongly adsorb to carbon and Pt electrodes. The measurements were performed over a range of potentials from -1.0 to -0.1 V in the case of MMF and pelargonin and 0 to 2.0 V in the case of protocatechuic acid, with a potential sweep rate of 200 mV/s. The compounds were dissolved in 5 mL of a solution of 0.1 M *tert*-butylammonium perchlorate in acetonitrile (MeCN) (100 μ L of 0.5 M HClO₄ was added to the anthocyanin solutions in order to guarantee that all of the anthocyanin was in the flavylium cation form). The CV of the supporting electrolyte solution was recorded first, and then, the anthocyanin was added and a new voltammogram recorded. The concentration of anthocyanin was in the range 0.1–1 mM in the voltammetric measurements and the protocatechuic acid was ~ 10 mM.

Fluorescence emission and excitation spectra were measured using a SPEX Fluorolog 212I spectrofluorimeter. All spectra were collected in the S/R mode and corrected for optics, detector wavelength dependence (emission spectra), and lamp intensity wavelength dependence (excitation spectra). Fluorescence was collected in right-angle geometry.

Time-resolved fluorescence measurements were carried out using the single-photon counting technique as described.¹⁶ The experimental instrumental response function for all excitation wavelengths was in the 38–42 ps range. Alternate collection of pulse profile and sample decays was performed (10³ counts at the maximum per cycle) until about 5 000–10 000 counts had been collected at the maximum of the fluorescence signal. Fluorescence decays were deconvoluted on a PC using George Striker's program.¹⁷

Semiempirical Calculations. Theoretical calculations were carried out on a personal computer using *HyperChem* version 5.0 software from Hypercube. Molecular geometries were first calculated using the MM⁺ molecular mechanics method and then optimized using the semiempirical AM1 method at the UHF level. The enthalpies of formation were obtained from single-point AM1 calculations at the optimized geometries. Theoretical gas-phase electron affinities (EAs) of the flavylium cation were calculated from the enthalpies of formation of AH⁺ and of its radical AH[•]

$$EA = \Delta H_f(\text{AH}^\bullet) - \Delta H_f(\text{AH}^+) \quad (1)$$

Similarly, the adiabatic gas-phase ionization potentials (IPs) of the polyphenolic electron donors were calculated from the

TABLE 1: Calculated Ionization Potential, IP, of Natural Copigments and Equilibrium Constant, K_C , for Complexation (Copigmentation) of Pelargonin (Pelargonidin 3,5-diglucoside) and MMF (With Dynamic Quenching Correction) at pH 0.25

copigment	IP/eV	K_C pelargonin	K_C MMF
		($E_{\text{Red}} = -0.346$ V vs SCE, MeCN)	($E_{\text{Red}} = -0.320$ V vs SCE, MeCN)
quercitrin	7.63	1737	1230
isoquercitrin	7.80	1050	734
ferulic acid	8.21	256	214
caffeic acid	8.32	237	186
gallic acid	8.61	87	102
protocatechuic acid	8.76	68	78 ^a

^a Determined at pH = 1.94.

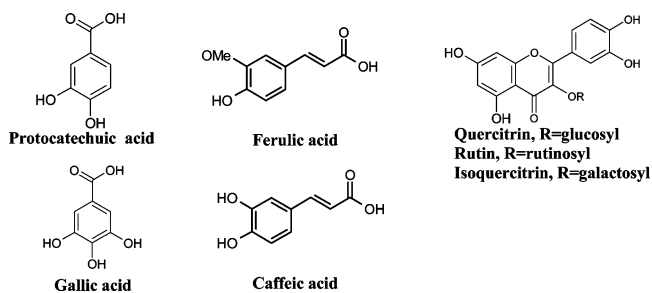
enthalpies of formation of the donor $\Delta H_f(\text{D})$ and of its radical cation $\Delta H_f(\text{D}^{\bullet+})$ (see Table 1)

$$IP = \Delta H_f(\text{D}^{\bullet+}) - \Delta H_f(\text{D}) \quad (2)$$

Results

Fluorescence Quenching of MMF by Phenols. Figure 1 shows absorption and fluorescence spectra ($\lambda_{\text{exc}} = 425$ nm, isosbestic excitation) of aqueous solutions (pH 1.94, HClO₄) of the synthetic model MMF in the presence of different concentrations of protocatechuic acid (PCA, Chart 2).

CHART 2



MMF neither hydrates nor deprotonates in water and, hence, exists only in the flavylium cation form.⁴ The absorption spectra exhibit alterations, upon increasing the concentration of PCA, that are indicative of complex formation (Figure 1a). Additionally, strong fluorescence quenching of MMF by PCA is observed (Figure 1b). The steady-state Stern–Volmer plot (I_0/I vs [PCA]) is shown in Figure 2.

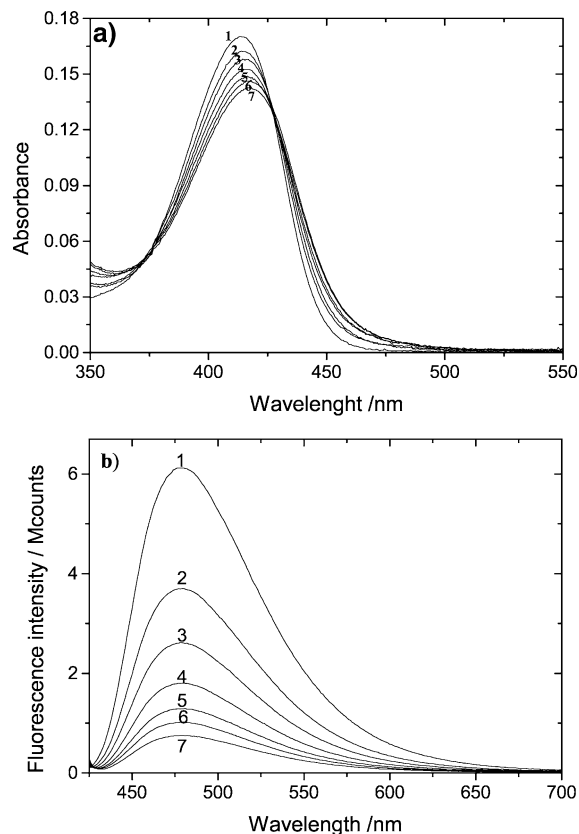


Figure 1. (part a) Absorption spectra of MMF (6.3×10^{-6} M) in aqueous solution at pH 1.94 as a function of the concentration of protocatechuic acid at 25 °C: (1) 0 M, (2) 5.0 mM, (3) 10.0 mM, (4) 15.1 mM, (5) 20.1 mM, (6) 25.1 mM, (7) 30.0 mM. (part b) Fluorescence spectra of the same solutions resulting from isosbestic excitation at 425 nm.

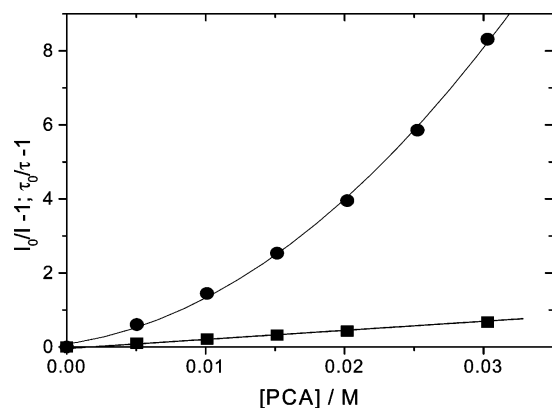


Figure 2. Steady-state (●) and time-resolved (■) Stern–Volmer plots of MMF in the presence of PCA, in water at pH 1.94, and at 25 °C. The solid lines represent fits of the I_0/I and τ_0/τ data with eqs 6 and 4, respectively.

The fluorescence decay of MMF in the absence of PCA is single-exponential with a lifetime equal to $\tau_0 = 4.67$ ns. Upon addition of PCA, single-exponential fits are still acceptable (see text to follow), and the decay time decreases down to $\tau = 2.80$ ns at 3.03×10^{-2} M PCA. The transient-state Stern–Volmer plot (τ_0/τ vs [PCA]), is also shown in Figure 2. The presence of static fluorescence quenching, due to direct excitation of ground-state complexes, is evident from the upward curvature of the steady-state plot and the much larger values of I_0/I as compared to those of τ_0/τ ($I_0/I = 9.32$ and $\tau_0/\tau = 1.67$ at the highest PCA concentration, 3.03×10^{-2} M).

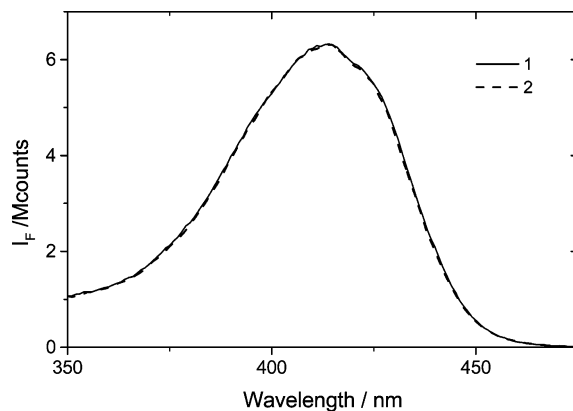


Figure 3. Fluorescence excitation spectra of MMF in aqueous solution at pH 1.94: (1) no copigment, (2) in the presence of 30 mM PCA. The spectra are identical.

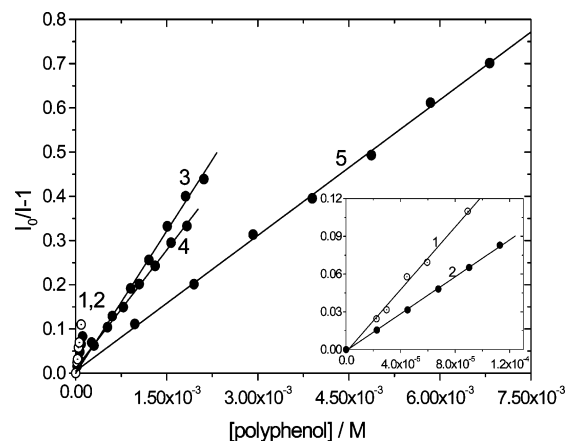


Figure 4. Steady-state Stern–Volmer plots of MMF in the presence of (1) quercitrin, (2) isoquercitrin, (3) ferulic acid, (4) caffeic acid, and (5) gallic acid in water at pH 0.25.

As shown in Figure 3, the quenching is dominated by static fluorescence quenching of complexed MMF. The excitation spectra of MMF are identical in the presence and absence of PCA, despite the fact that the absorption spectra of the solutions are red-shifted in the presence of PCA (see Figure 1a). This means that only the uncomplexed MMF contributes significantly to the fluorescence emission.

Because static quenching indicates the presence of a process or processes that occur in a time range that is shorter than the time resolution of the equipment, we have searched for fast components in the fluorescence decay of the 3.03×10^{-2} M solution, using 1.214 ps/channel resolution. Even with this time resolution, no evidence for such an ultrafast component was observed.

Absorption and fluorescence data of MMF in the presence of the polyphenols quercitrin, isoquercitrin, ferulic acid, caffeic acid, and gallic acid (Chart 2) show a pattern similar to that observed in the presence of PCA: ground-state complex formation, as evidenced by the absorption spectra, and strong static quenching of the fluorescence. For these polyphenols, however, curvature was not observed in the I_0/I Stern–Volmer plots over the concentration range permitted by the much lower water solubility of these compounds (Figure 4). At these low concentrations, dynamic quenching was negligible for quercitrin and isoquercitrin ($\tau_0/\tau \approx 1$ at 0.09 and 0.11 mM, respectively) and τ_0/τ is much less than I_0/I for ferulic acid ($\tau_0/\tau = 1.05$ vs $I_0/I = 1.44$ at 2.06 mM) and caffeic acid ($\tau_0/\tau = 1.06$ vs $I_0/I = 1.35$ at 1.75 mM).

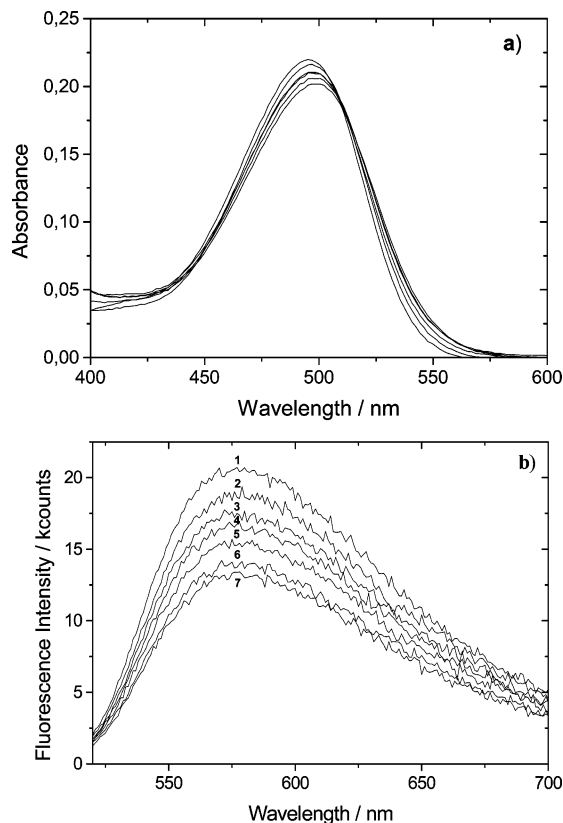


Figure 5. (part a) Absorption spectra of pelargonin in aqueous solution at pH 0.25, as a function of the concentration of ferulic acid at 25 °C: (1) no copigment, (2) 0.36 mM, (3) 0.71 mM, (4) 1.07 mM, (5) 1.43 mM, (6) 1.78 mM, (7) 2.14 mM. (part b) Fluorescence spectra of the same solutions ($\lambda_{\text{exc}} = 510$ nm, isosbestic excitation).

Fluorescence Quenching of Pelargonin by Phenols. Absorption and emission spectra of pH 0.25 (HClO_4) aqueous solutions of the natural anthocyanin pelargonin (PLG) in the presence of different concentrations of ferulic acid (FRA) are shown in Figure 5. Pelargonin undergoes all the reactions shown in Scheme 1, but only the AH^+ form exists at pH 0.25 in the ground state. Ground-state complex formation between the AH^+ form of PLG and FRA is also evident from the changes in the absorption spectra upon increasing the FRA concentration (Figure 5a).

The fluorescence spectrum of PLG ($\lambda_{\text{exc}} = 510$ nm, isosbestic point) is shown in Figure 5b. The spectrum has been shown to be composed of two strongly overlapped emission bands: one corresponding to the excited flavylium cation (AH^+) * and the other to the excited base A^* formed via adiabatic deprotonation of (AH^+) * .⁵ Addition of FRA results in strong fluorescence quenching, as observed with MMF. The normalized excitation spectra (not shown) of these solutions ($\lambda_{\text{em}} = 580$ nm) are independent of [FRA] and identical to the absorption spectrum of PLG in the absence of FRA. This is in contrast to the absorption spectra of the same solutions, which do show [FRA]-dependent changes, indicating that the complex between FRA and the AH^+ form of PLG does not contribute to the fluorescence at 580 nm.

The fluorescence decays of PLG in water, measured at several emission wavelengths and pH values, are double exponential due to the fast proton transfer from the excited AH^+ cation to water.⁵ The preexponential factor of the shorter decay time (ca. 20 ps at pH 1) is positive at the onset of the emission band (decay of excited AH^+) and negative at wavelengths longer than 530 nm (formation of the excited conjugate base A^*). The

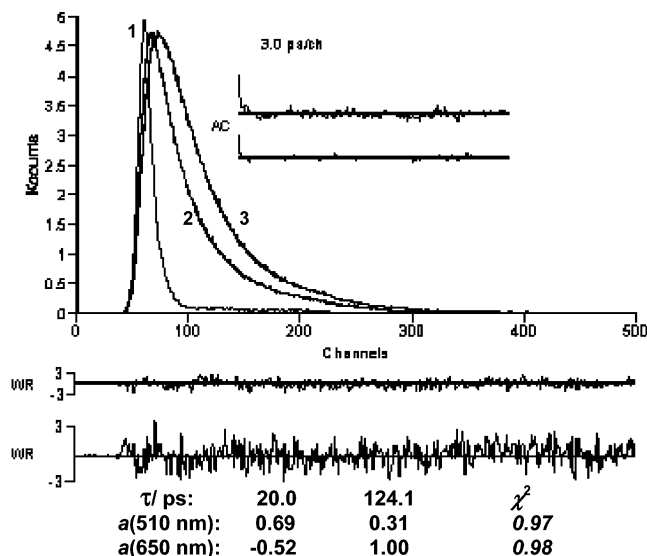


Figure 6. Fluorescence decays of pelargonin in aqueous solution at pH 0.25 in the presence of 2.15 mM ferulic acid, measured at the onset ($\lambda_{\text{em}1} = 510$ nm, curve 2) and the tail ($\lambda_{\text{em}2} = 650$ nm, curve 3) of the emission band. Curve 1 is the instrument response at 3 ps/channel. Results of global analysis of the decays with a sum of two exponentials (decay times, τ 's; preexponential coefficients, a 's; weighted residuals, WRs, and autocorrelation functions, ACs) are also shown. The shortest time (20 ps) appears as decay time at 510 nm and as rise time at 650 nm.

preexponential coefficient of the longer time (124 ps at pH 1) is positive at all wavelengths and represents the decay of A^* .⁵ At the band maximum (580 nm), the base form is responsible for essentially all of the fluorescence.

In contrast to the fluorescence quantum yields, the fluorescence decay of PLG in water at pH 0.25 is independent of the presence of FRA (i.e., dynamic quenching is not observed even at the highest [FRA] of 2.15×10^{-3} M) (Figure 6). This is not a particularly surprising result, because the longer decay time of pelargonin ($\tau_1 = 124$ ps) is very short (see Discussion). Therefore, the observed fluorescence quenching (Figure 5b) is entirely static in nature and the steady-state Stern–Volmer plot is linear (Figure 7a). Entirely analogous observations were made for PLG in the presence of quercitrin, isoquercitrin, ferulic acid, caffeic acid, and gallic acid (Figure 7b).

The fact that the fluorescence of the base form at 580 nm exhibits static quenching implies that the rate constant for nonradiative deactivation of the excited AH^+ –FRA complex is greater than k_d for the excited-state deprotonation of the flavylium cation of PLG ($k_d = 4.3 \times 10^{10} \text{ s}^{-1}$).⁵

Redox Properties of Anthocyanins and Polyphenols. Cyclic voltammograms of the AH^+ form of MMF and PLG were measured in acidified MeCN, as described in the Experimental Section. Irreversible reduction waves were observed (Figure 8a–b) at slightly negative potentials (voltage peaks at -0.32 and -0.29 V against SCE, respectively). In both cases, after some time, a second reduction peak appeared at somewhat more negative potentials (ca. -640 mV), the intensity of which increased with time at the expense of the first peak. Repetition of the voltammogram with a fresh Hg drop reproducibly yielded the first peak. These results are consistent with the assignment of the peak at ca. -640 mV to time-dependent adsorption onto the drop surface. The range of values observed by us for several anthocyanins (-0.29 to -0.40 V against SCE) is in accord with polarographic data reported in the literature^{18,19} for other flavylium cations, confirming that the AH^+ form of anthocyanins is quite readily reduced.

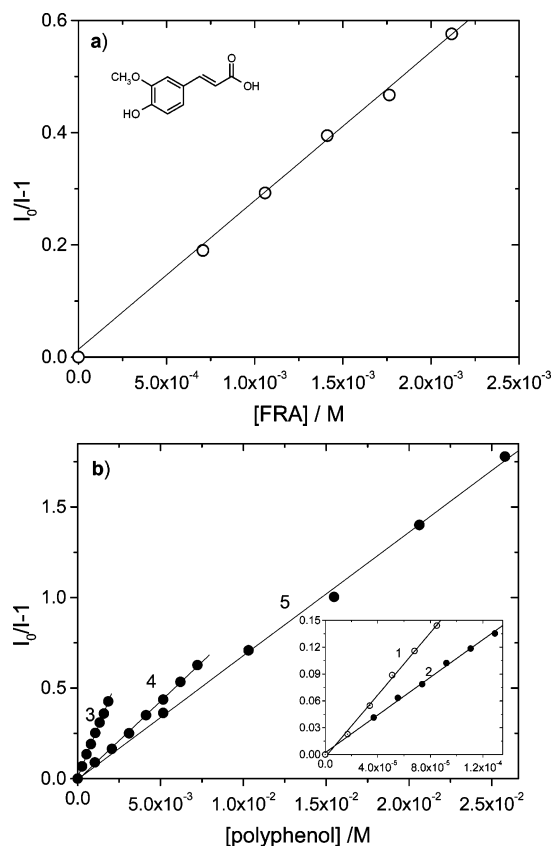


Figure 7. Steady-state Stern–Volmer plots of pelargonin in aqueous solution pH 0.25 in the presence of (part a) ferulic acid and (part b) (1) quercitrin, (2) isoquercitrin, (3) caffeic acid, (4) gallic acid, and (5) protocatechuic acid.

Accurate determination of one-electron oxidation potentials for polyphenols by CV is usually a complex task. In water, the complexity usually arises from the presence of multielectron processes and the coupling of proton and electron transfer processes.²⁰ In organic solvents such as acetonitrile or dimethyl sulfoxide, one-electron peaks can, however, be obtained, as exemplified by the reduction of anthocyanins in acetonitrile shown in Figure 8a–b and the oxidation of protocatechuic acid shown in Figure 8c. An alternative approach for determining one-electron oxidation potentials is to use pulse radiolysis to promote electron transfer to an acceptor of known redox potential. Several published values exist for polyphenols,²¹ but unfortunately, most of the data are obtained in water at pH = 7, where hydroxybenzoic or hydroxycinnamic acids exist mainly as hydroxybenzoates or hydroxycinnamates, respectively. Nonetheless, literature values of the redox potentials of ferulic acid (0.95 V vs SCE in MeCN)²⁰ and caffeic acid (0.85 V vs SCE in DMSO)²⁰ and our own value for the oxidation of protocatechuic acid (1.34 V vs SCE in MeCN) show an excellent linear correlation with calculated ionization potentials (see text to follow).

For correlation purposes, theoretical gas-phase EAs of the flavylum cation from AH⁺ of pelargonin and MMF were calculated from the enthalpies of formation of AH⁺ and the neutral radical AH[•] (see Experimental Section). The values are nearly the same (within 0.1 eV of each other) for these two anthocyanins and are extraordinarily large (EA(PLG) = 6.91 eV and EA(MMF) = 6.83 eV), even when compared to gas-phase EA values of good electron acceptors such as tetracyanoethene (EA = 3.2 eV).²² We have also calculated theoretical EAs by an analogous procedure for 23 related compounds for which experimental EAs are available.²² Our calculated values

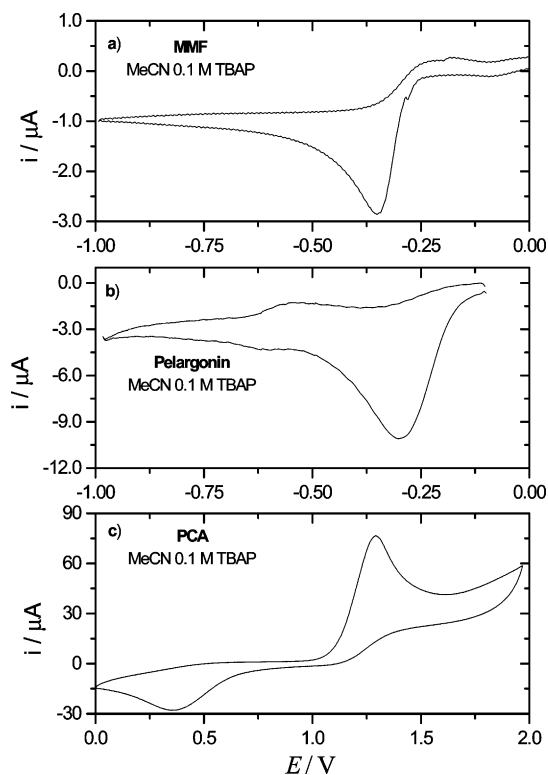


Figure 8. Cyclic voltammograms of (a) MMF (vs SCE), (b) pelargonin (vs Ag/AgCl), and (c) protocatechuic acid (vs SCE) in acetonitrile at 25 °C.

are systematically larger than the experimental ones by a mean value of ca. 0.65 eV, with a deviation never greater than 1.15 eV (EA(exptl) = 1.06 × EA(calcd) – 0.65 ± 0.3 eV). On this basis, a lower limit value of 5.8 eV for the gas-phase EA of AH⁺ may be set. This supports the electrochemical data in the prediction that AH⁺ is an unusually good electron acceptor, even in water, where EA should be reduced by an amount corresponding to the free energy of transfer from the gas phase to water (which can be estimated to be ca. 1.7 eV by the Born approach, eq 3).

$$\text{EA}(\text{water}) = \text{EA}(\text{gas phase}) - \frac{\epsilon - 1}{2\epsilon} \cdot \frac{e^2}{r_{\text{AH}^+}} \quad (3)$$

The calculated gas-phase EA values of the base (2.29 eV), hemiacetal (1.42 eV), and chalcone (0.60 eV) forms of PLG and other anthocyanins are much lower than that of the acid form.

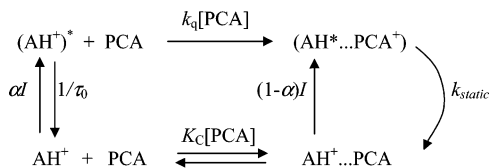
Gas-phase IPs of the polyphenols quercitrin, isoquercitrin, ferulic acid, caffeic acid, gallic acid, and protocatechuic acid were also estimated (Table 1) from the difference between the calculated enthalpies of formation of the polyphenol radical cation and the polyphenol itself, as described in the Experimental Section. In the case of IPs, the agreement between the calculated values (from formation enthalpies) and available experimental gas-phase ionization energies (NIST database²²) is much better than in the case of EAs, with deviations always smaller than 0.5 eV. A similar observation has been made by other authors.²³

The IP values range from 7.63 to 8.76 eV. The lowest values were found for the flavones (e.g., quercitrin and isoquercitrin), and are similar to the IP values of typical good electron donors (e.g., triethylamine, 7.50 eV, or *N*-methylaniline, 7.33 eV).²² Intermediate values were obtained for the cinnamic acid derivatives, and the benzoic acids were the poorest electron donors considered.

Discussion

Mechanism and Kinetics of Fluorescence Quenching of MMF. The mechanism of mixed static and dynamic quenching processes is shown in Scheme 2, where K_C represents the equilibrium constant for ground-state complexation, k_q is the dynamic quenching rate constant, τ_0 is the unquenched fluorescence lifetime of the MMF cation, $\alpha = 1/(1 + K_C[\text{PCA}])$ is the mole fraction of uncomplexed MMF cation, and k_{static} the rate constant for static quenching in the complex.

SCHEME 2



The observation of single exponential decays means that the quenching process is irreversible in practice. Under irreversibility conditions, the transient-state Stern–Volmer plot (τ_0/τ vs $[\text{PCA}]$), shown in Figure 2) obeys eq 4, from which the value of $k_q = 4.6 \times 10^9 \text{ M}^{-1} \text{ s}^{-1}$ is obtained for the bimolecular quenching rate constant of MMF by PCA. This value is close to the diffusion-controlled limit in water at 20 °C ($k_{\text{diff}} = 6 \times 10^9 \text{ M}^{-1} \text{ s}^{-1}$ from $k_{\text{diff}} = 8RT/3000\eta$, where η is the viscosity).²⁴ Values close to the diffusion limit were also obtained for caffeic and ferulic acids ($k_q = 7.2 \times 10^9 \text{ M}^{-1} \text{ s}^{-1}$ and $k_q = 5.5 \times 10^9 \text{ M}^{-1} \text{ s}^{-1}$, respectively).

$$\frac{\tau_0}{\tau} = 1 + k_q \tau_0 [\text{PCA}] \quad (4)$$

The absence of an ultrafast component in the fluorescence decays of MMF in the presence of PCA means that the static process occurs on a time scale that is shorter than the resolution of our apparatus (ca. 3 ps).¹⁶ We conclude, therefore, that the static quenching must be faster than the reciprocal of our time resolution, which places a lower limit of ca. 10^{11} s^{-1} on k_{static} in Scheme 2.

Scheme 2 predicts the following steady-state Stern–Volmer relationship (eq 5)

$$\frac{I_0}{I} = (1 + k_q \tau_0 [\text{PCA}]) \cdot (1 + K_C [\text{PCA}]) = \frac{\tau_0}{\tau} \cdot (1 + K_C [\text{PCA}]) \quad (5)$$

However, when $(I_0/I)/(\tau_0/\tau)$ is plotted against $[\text{PCA}]$, an upward curvature is still observed. This suggests that a second complexation occurs. If the subsequent formation of a 1:2 complex is included in Scheme 2, eq 6 is obtained

$$\frac{I_0}{I} = (1 + k_q \tau_0 [\text{PCA}]) \cdot \{1 + K_{C1} [\text{PCA}] + (1 + K_{C2} [\text{PCA}])\} \quad (6)$$

The plot of $[(I_0/I)/(\tau_0/\tau) - 1]/[\text{PCA}]$ versus $[\text{PCA}]$ is indeed linear, yielding the value of the equilibrium constant of the 1:1 complex from the intercept ($K_{C1} = 78 \text{ M}^{-1}$) and that of the 1:2 complex from the slope/intercept ratio ($K_{C2} = 28 \text{ M}^{-1}$). The value of K_{C1} is only slightly smaller than the value of $K_C = 89 \text{ M}^{-1}$ that is obtained when eq 6 (which neglects the formation of the 1:2 complex) is fitted to the data in the low-concentration range.

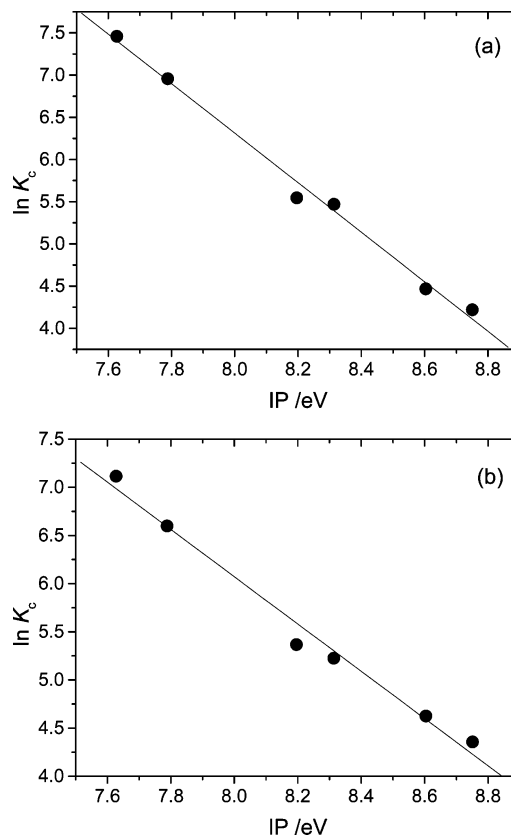


Figure 9. Correlation of the logarithm of the equilibrium constant for complexation, K_C , with the calculated ionization potential, IP, of the polyphenol (quercitrin, isoquercitrin, gallic acid, ferulic acid, caffeic acid, and protocatechuic acid) for (part a) MMF and (part b) pelargonin.

In the cases of quercitrin, isoquercitrin, gallic acid, ferulic acid, and caffeic acid, which are much less water soluble than PCA, the polyphenol concentrations were never high enough to produce a significant amount of 1:2 complex, and deviations from eq 5 were not observed. The values of the equilibrium constants for complexation of MMF by the polyphenols studied here are collected in Table 1. Clearly, the determination of K_C from eq 5 or 6 is straightforward and provides a new method for the evaluation of the so-called copigmentation constants^{11,12} of anthocyanins without the approximations involved in the usual absorption spectroscopic methods.¹¹

Nature of the Ground-State Complexes of MMF with Polyphenols and of the Static Quenching Process. Figure 9a shows a plot of the logarithm of K_C values for the monocomplexation of MMF by the polyphenols versus the IP of the polyphenol. The linearity of the plot indicates that the Gibbs energy of complexation is directly proportional to the IP of the polyphenol. This, together with the magnitude of $\text{IP}_{\text{poly}} - \text{EA}_{\text{MMF}}$ (ranging from 0.81 eV for quercitrin to 1.98 eV for PCA), strongly suggests a charge transfer nature for the MMF–polyphenol ground-state complexes, with the polyphenol acting as the electron donor and MMF as the electron acceptor.

From the fluorescence intensity and lifetime measurements, the lower limit on the rate constant for static quenching of MMF by PCA, k_{static} , was estimated to be $\geq 10^{11} \text{ s}^{-1}$, while that for dynamic quenching, k_q , is diffusion-controlled ($4.6 \times 10^9 \text{ M}^{-1} \text{ s}^{-1}$). Among processes known to occur at such a high rate, electron transfer is the obvious choice, because alternative processes, such as proton or energy transfer, can be excluded in this system, because MMF has no acidic protons and absorbs at longer wavelengths than PCA.

The standard Gibbs free energy for excited-state electron transfer in water ΔG^* can be evaluated from eq 7,²⁵

$$\Delta G^* = E_{\text{ox}} - E_{\text{red}} + \Delta\Delta G_{\text{solv}} + \Delta G_{\text{Coul}} - E_{\text{oo}} + \Delta G^\circ \quad (7)$$

where $\text{IP} - \text{EA}$ is replaced by $E_{\text{ox}} - E_{\text{red}}$, the numeric difference between the oxidation potential of the electron donor and the reduction potential of the electron acceptor in a given solvent (e.g., MeCN) and $\Delta\Delta G_{\text{solv}}$ is a correction for the difference between $E_{\text{ox}} - E_{\text{red}}$ in that solvent and in water (in eV). ΔG_{Coul} represents the difference in the free energies of approximation of the products (AH^- and PCA^+) and reactants (AH^+ and PCA) in water. $E_{\text{oo}} = 2.88$ eV is the excitation energy of MMF in water, taken from the onset of the emission spectrum (430 nm), and $\Delta G^\circ = -RT \ln K_C$ is the free energy of complex formation in the ground state.

In the present case, both the reactants and products consist of a cation plus a neutral species, and the redox potentials were determined in a suitably polar solvent (CH_3CN). Consequently, both ΔG_{solv} and $\Delta\Delta G_{\text{solv}}$ can be safely assumed to be negligible. Thus, for the MMF-PCA pair, we estimate the value of ΔG^* to be ca. -1.14 eV ($\Delta G^* = 1.34 + 0.29 - 2.88 + 0.11$). Taking a value of $\lambda = 1.6$ eV²⁶ for the repolarization energy in water, the free energy of activation for electron transfer (eq 8)²⁷ is estimated to be ca. 0.033 eV. Assuming a value of $k_{\text{ET}}^\circ = 10^{12}$ s⁻¹ (equal to the reciprocal dielectric relaxation time of water), the rate constant for electron transfer should be ca. 3×10^{11} s⁻¹ (eq 9), larger than the experimental lower limit of 10^{11} s⁻¹. Therefore, ultrafast electron transfer is the most plausible mechanism for the static quenching of the fluorescence of MMF by PCA (i.e., $k_{\text{static}} = k_{\text{ET}}$).

$$\Delta G^\ddagger = \frac{(\Delta G^* + \lambda)^2}{4\lambda} = 0.033 \text{ eV} \quad (8)$$

$$k_{\text{ET}} = k_{\text{ET}}^\circ \exp\left(\frac{-\Delta G^\ddagger}{RT}\right) \quad (9)$$

Excited-State Electron Transfer and Ground-State Complex Formation with PLG. The AH^+ forms of PLG and all natural anthocyanins are super photoacids.^{4,5} The excited-state deprotonation rate constants of AH^+ to water are on the order of $0.4\text{--}2 \times 10^{11}$ s⁻¹ (4.3×10^{10} s⁻¹ in the case of PLG).⁵ Thus, a bimolecular diffusion-controlled reaction can only compete with deprotonation at quencher concentrations above 1 M. In the case of PLG and FRA, the concentrations of FRA are less than 2×10^{-3} M, and the contribution of dynamic quenching is completely negligible. Under these conditions, eq 5 reduces to eq 10 and the steady-state Stern-Volmer plots for the quenching of PLG fluorescence are linear with a slope equal to K_C , the equilibrium constant for complexation of PLG by the polyphenol (Table 1).

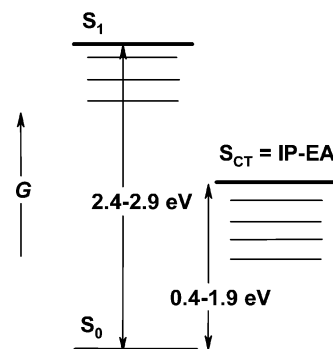
$$\frac{I_0}{I} = 1 + K_C [\text{FRA}] \quad (10)$$

In Figure 9b, the values of $\log K_C$ are plotted against the ionization potential of the polyphenol. The plot is linear and similar to that obtained for MMF, as expected from the similar electron affinities and reduction potentials of the two anthocyanins. There are, in principle, two competitive paths for quenching of the excited PLG-FRA complex: electron transfer from FRA to PLG (k_{static}) and deprotonation to water ($k_d = 4.3 \times 10^{10}$ s⁻¹ in the absence of FRA)⁵ to give the base. As already noted (vide supra), the efficient static fluorescence quenching

of the base form at 580 nm implies that $k_{\text{static}} > k_d$. Indeed, calculation of the standard free energy for the excited-state electron transfer from eq 7, employing the values $E_{\text{ox}}(\text{FRA}) = 0.95$ V,²⁰ $E_{\text{red}}(\text{PLG}) = -0.32$ V, $E_{\text{oo}}(\text{PLG}) = 2.41$ eV (515 nm), and $\Delta G^\circ = -0.14$ eV provides a value of $\Delta G^* = -1.00$ eV, compatible with an electron transfer rate constant in the range of ca. 1×10^{11} s⁻¹, confirming that $k_{\text{ET}} \gg k_d$.

Chart 3 shows a gas-phase state diagram for the twelve MMF-polyphenol and PLG-polyphenol complexes studied here. In all cases, the charge transfer state S_{CT} energy is substantially lower than the first singlet excited state of AH^+ . Given the similarity of values of electron affinities and reduction potentials of the cationic form (AH^+) of most anthocyanins, this conclusion is probably extensible to all flavylium salts.

CHART 3



Conclusions

The first conclusion of the present study is that both the synthetic and natural anthocyanins MMF and PLG form ground-state complexes with a number of natural polyphenols, with the main driving force for complexation being charge transfer from the polyphenol to the cationic form of the anthocyanin.

The second conclusion is that excitation of these anthocyanin-polyphenol charge transfer complexes leads to ultrafast electron transfer from the copigment to the anthocyanin, with a rate constant faster than 10^{11} s⁻¹. As a consequence of its high reduction potential, the excited singlet state of the flavylium cation form of anthocyanins should be capable of oxidizing most polyphenols, as well as biomolecules such as tyrosine ($\text{IP} = 8.4$ eV) and tryptophan ($\text{IP} = 7.5$ eV).

Why, then, does nature allow the presence of the potentially deleterious consequences of this strong photooxidizing power of the anthocyanins present in flowers, fruits, and, in some cases, leaves upon absorption of solar radiation? Anthocyanins have been implicated in the protection of plant tissues against an excess of solar radiation,²⁸ and in favor of this function are the facts that the flavylium cation forms of natural anthocyanins strongly absorb green light ($\epsilon_{500\text{ nm}} \approx 4 \times 10^4$ M⁻¹ cm⁻¹), which is not absorbed by chlorophyll, and are super-photoacids (excited-state $\text{p}K_a < 0$),^{4,5} with a quantum efficiency of proton transfer to water greater than 0.99. Thus, in uncomplexed anthocyanins, ultrafast proton transfer appears to be the major pathway for fast nonradiative deactivation of the excited state.

In plant vacuoles, anthocyanins also often coexist with polyphenols,¹⁴ and the persistence of the red color indicates that the flavylium ion is complexed with these polyphenols. In flavylium cation-polyphenol complexes, our results point to ultrafast electron transfer, rather than proton transfer, as the major primary process. This coexistence is a potential source of free radicals if recombination is not 100% efficient and might

eventually have implications for the in vivo role of anthocyanin–polyphenol complexes.

Acknowledgment. This work was supported by Fundação para a Ciência e Tecnologia (FCT), Portugal (project POCTI/QUI/38884/2001), FAPESP, Brasil, and ICCTI/CAPES/423. F.H.Q. thanks the Conselho Nacional de Desenvolvimento Científico e Tecnológico (CNPq) for fellowship support.

References and Notes

- (1) Swain, T. Evolution of flavonoid compounds. In *The Flavonoids*; Harborne, J. B., Mabry, T. J., Mabry, H., Eds.; Chapman and Hall: London, 1975; p 1129.
- (2) Harborne, J. B.; Williams, C. A. *Phytochemistry* **2000**, *55*, 481.
- (3) Kondo, T.; Ueda, M.; Isobe, M.; Goto, T. *Tetrahedron Lett.* **1998**, *39*, 8307.
- (4) Lima, J. C.; Abreu, I.; Santos, M. H.; Brouillard, R.; Maçanita, A. L. *Chem. Phys. Lett.* **1998**, *298*, 189.
- (5) Moreira, P. F., Jr.; Giestas, L.; Yihwa, C.; Vautier-Giongo, C.; Quina, F. H.; Maçanita, A. L.; Lima, J. C. *J. Phys. Chem. A* **2003**, *107*, 4203.
- (6) Brouillard, R.; Dubois, J. E. *J. Am. Chem. Soc.* **1977**, *99*, 1359.
- (7) Brouillard, R.; Delaporte, B. *J. Am. Chem. Soc.* **1977**, *99*, 8461.
- (8) Santos, H.; Turner, D. L.; Lima, J. C.; Figueiredo, P.; Pina, F.; Maçanita, A. L. *Phytochemistry* **1993**, *33*, 1227.
- (9) Pina, F.; Benedito, L.; Melo, M. J.; Parola, A. J.; Lima, J. C.; Maçanita, A. L. *An. Quím. Int. Ed.* **1997**, *93*, 111.
- (10) Mazza, G.; Brouillard, R. *Food Chem.* **1987**, *25*, 207.
- (11) Wigand, M. C. Étude par Spectroscopie Electronique de l'Interaction Moleculaire dite de Copigmentation. Ph. D. Thesis, Université Louis Pasteur, Strasbourg, 1991.
- (12) Baranac, J. M.; Petranovic, N. A.; Dimitric-Markovic, J. M. *J. Agric. Food Chem.* **1996**, *44*, 133; **1997**, *45*, 1694, 1698, 1701.
- (13) Saito, N.; Osawa, Y.; Hayashi, K. *Phytochemistry* **1971**, *10*, 445.
- (14) Mazza, C. A.; Boccalandro, H. E.; Geordano, C. V.; Battista, D.; Scopel, A. L.; Ballaré, C. L. *Plant Physiol.* **2000**, *122*, 117.
- (15) Houbiers, C.; Lima, J. C.; Santos, M. H.; Maçanita, A. L. *J. Phys. Chem.* **1998**, *102*, 3578.
- (16) Giestas, L.; Yihwa, C.; Lima, J. C.; Vautier-Giongo, C.; Lopes, A.; Quina, F. H.; Maçanita, A. L. *J. Phys. Chem. A* **2003**, *107*, 3263.
- (17) Striker, G.; Subramaniam, V.; Seidel, C. A. M.; Volkmer, A. J. *J. Phys. Chem. B* **1999**, *103*, 8612.
- (18) Harper, K. A.; Chandler, B. V. *Aust. J. Chem.* **1967**, *20*, 731.
- (19) Harper, K. A. *Aust. J. Chem.* **1968**, *21*, 221.
- (20) Hapiot, P.; Neudeck, A.; Pinson, J.; Fulcrand, H.; Neta, P.; Rolando, C. *J. Electroanal. Chem.* **1996**, *405*, 169.
- (21) Jovanovic, S. V.; Steenken, S.; Tosic, M.; Marjanovic, B.; Simic, M. G. *J. Am. Chem. Soc.* **1994**, *116*, 4846.
- (22) Lias, S. G.; Bartmess, J. E.; Liebman, J. F.; Holmes, J. L.; Levin, R. D.; Mallardin, W. G.; Lias, S. G.; Levin, R. D.; Kafafi, S. A. Ion Energetics Data. In *NIST Chemistry WebBook, NIST Standard Reference Database Number 69*; Linstrom, P. J., Mallard, W. G., Eds.; National Institute of Standards and Technology: Gaithersburg, MD. <http://webbook.nist.gov> (accessed July 2004).
- (23) Dewar, M. J. S.; Zoedisch, E. G.; Healy, E. F.; Stewart, J. J. P. *J. Am. Chem. Soc.* **1985**, *107*, 3902.
- (24) Alwattar, A. H.; Lumb, M. D.; Birks, J. B. In *Organic Molecular Photophysics*; Birks, J. B., Ed.; Wiley-Interscience: 1973; Vol. 1, p 403.
- (25) Weller, A. In *The Exciplex*; Gordon, M., Ware, W. R., Eds.; Academic Press: New York, 1975; p 23.
- (26) Wiczak, W.; Rzeska, A.; Lukomska, J.; Stachowiak, K.; Karolczak, J.; Malicka, J.; Lankiewicz, L. *Chem. Phys. Lett.* **2001**, *341*, 99.
- (27) Marcus, R. A. *J. Chem. Phys.* **1965**, *43*, 679.
- (28) Steyn, W. J.; Wand, S. J. E.; Holcroft, D. M.; Jacobs, G. *New Phytol.* **2002**, *155*, 349.